EUROPEAN FUSION DEVELOPMENT AGREEMENT

EFDA–JET–CP(04)03-62

K-D Zastrow J.M. Adams, Yu Baranov, P. Belo, L. Bertalot, J.H. Brzozowski, C.D. Challis, S. Conroy, M de Baar, P de Vries, P. Dumortier, J. Ferreira, L. Garzotti, T.C. Hender, E. Joffrin, V. Kiptily, J Mailloux, D.C. McDonald, R. Neu, M.O'Mullane, M.F.F. Nave, J. Ongena, S. Popovichev, M. Stamp, J. Stober, D Stork, I. Voitsekhovitch , M. Valovic, H. Weisen, A.D. Whiteford, A. Zabolotsky and JET EFDA Contributors

Tritium Transport Experiments on the JET Tokamak

Tritium Transport Experiments on the JET Tokamak

K-D Zastrow[1], J.M. Adams[1], Yu Baranov[1], P. Belo[2], L. Bertalot[3], J.H. Brzozowski[4], C.D. Challis[1], S. Conroy[5], M de Baar[6], P de Vries[1], P. Dumortier[7], J. Ferreira[2], L. Garzotti[8], T.C. Hender[1], E. Joffrin[9], V. Kiptily[1], J Mailloux[1], D.C. McDonald[1], R. Neu[10], M.O'Mullane[11], M.F.F. Nave[2], J. Ongena[7], S. Popovichev[1], M. Stamp[1], J. Stober[10], D Stork[1], I. Voitsekhovitch[11], M. Valovic[1], H. Weisen[12], A.D. Whiteford[11], A. Zabolotsky[12] and JET EFDA Contributors*

[1]EURATOM/UKAEA Fusion Association, Culham Science Centre, Abingdon, OX14 3DB, UK
[2]EURATOM/IST Fusion Association, Lisboa, Portugal
[3]Associazione EURATOM-ENEA sulla Fusione, Frascati, Italy.
[4]Alfvén Laboratory, EURATOM-VR Asociation, Stockholm, Sweden.
[5]Dept. of Neutron Research, Uppsala University, EURATOM-VR Asociation, Uppsala, Sweden.
[6]FOM Instituut voor Plasmaphysica, Associatie Euratom, Nieuwegein, The Netherlands.
[7]Association EURATOM-Belgian State, ERM-KMS, Brussels, Belgium
[8]Consorzio-RFX, Associazione EURATOM-ENEA sulla Fusione, Padova, Italy.
[9]Association EURATOM-CEA sur la Fusion, CEA Cadarache, St Paul-lez Durance, France
[10]Max-Planck Institut für Plasmaphysik, EURATOM Assoziation, Garching, Germany
[11]Dept. of Physics, University of Strathclyde, Glasgow, United Kingdom
[12]CRPP-EPFL, Association EURATOM-Confédération Suisse, Lausanne, Switzerland
** See annex of J. Pamela et al, "Overview of Recent JET Results and Future Perspectives", Fusion Energy 2002 (Proc. 19th IAEA Fusion Energy Conference, Lyon (2002).*

Preprint of Paper to be submitted for publication in Proceedings of the
31st EPS Conference,
(London, UK. 28th June - 2nd July 2004)

INTRODUCTION

From particle transport studies on deuterium ions in steady-state plasmas, only the ratio of convection, v_D, to diffusion, D_D, can be measured since the dominant source (which is only poorly characterized experimentally) and the sink are both at the edge. This is in addition to the difficulty that fuel ion densities cannot be measured directly but have to be inferred from quasi-neutrality, using electron and impurity density measurements. The time evolution of the tritium spatial distribution, on the other hand, can be detected even in "trace" quantities by observation of the 14MeV neutron emission (typically $n_T / (n_D + n_T) < 3\%$ are used in our experiments) which allows transient experiments using a fuel ion species without perturbation of the background plasma. Thus, "trace tritium" experiments allow vT and DT to be measured separately. Previous "trace tritium" experiments have been conducted on JET in 1991 and 1997 [24, 20, 9] and on TFTR in 1993 [5, 6].

We have performed tritium transport studies in all ITER operational regimes as part of the 2003 JET Trace Tritium Experiment (TTE) [14]. We studied ELMy H-Mode plasmas, hybrid scenario discharges [13] and weak and strong Internal Transport Barrier (ITB) discharges [27, 3] in dedicated experiments. The electron density was varied from the natural density, i.e. relying only on beam fuelling and wall recycling, to the Greenwald density [7] with strong external gas fuelling. Plasma current as well as toroidal field were varied over a wide region covering q_{95} from 3 to 6. For this paper, we present the results obtained so far after the analysis of twenty-two representative discharges.

In section 2 of this paper, we give a brief overview of the experimental technique and the method to derive v_T and D_T. A more detailed description is beyond the scope of this paper. In section 3 we present observations on the spatial profile of the neutron emission due to the reaction partner distribution (fast deuterium ions from neutral beam injecton) and of transport due to MHD driven events (sawtooth collapses, Neo-classical Tearing Modes (NTM) and Edge Localized Modes (ELM)). Conditions under which tritium transport is reduced to levels consistent with neo-classical theory and the scaling of tritium transport above neo-classical levels with engineering and local physics parameters is discussed in Section 4. Conclusions based on the analysis of this subset of data from the TTE campaign are presented in Section 5.

1. EXPERIMENTAL TECHNIQUE AND ANALYSIS METHOD

The neutron emission from DD and DT reactions is measured on JET with a nineteen-channel neutron profile monitor and by measurement of the total neutron rate [18, 23]. The profile monitor has ten horizontal (#1-#10) and nine vertical (#11-#19) lines-of-sight; these are overlayed on the emissivity contours shown in Fig.3. Both sets of diagnostics are absolutely calibrated at 2.5MeV for DD and 14MeV for DT reactions, and provide 10 msec time resolution. The outermost channel of the profile monitor (#10) has an impact parameter with the plasma axis of $r/a = 0.91$ for typical JET discharges, while the outermost channels with good statistics are channels #9 and #19, with typically $r/a = 0.82$. We can therefore regard the plasma region inside $r/a \approx 0.85$ as the region observed by this diagnostic, with no experimental information on tritium density available outside this region except for small contributions to the neutron yield with low reactivity but large volume.

The data from the neutron profile monitor and neutron yield are analysed by least-squares fitting of a transport model for tritium with free parameters for the spatial profiles of D_T and v_T and the influx. We use the $1^1/_2$-D impurity transport code SANCO [17] for this study. The transport coefficients are assumed to be constant in time for ELMy H-Mode and hybrid scenario discharges, whereas radial movement of transport barriers is allowed for ITB discharges. Neutral transport and losses by charge-exchange with cold edge neutrals and fast beam neutrals are included in the model. The tritium ion density calculated by the transport model is post-processed to derive the line integrals of the 2.5MeV and 14MeV neutron emissivity, and these ideal line integrals are in turn post-processed to take the scattering of neutrons in the collimator and other parts of the vessel into account. The coefficients that describe the 2D profile of the neutron emissivity, and the coefficients for neutral transport, are derived for each discharge using the TRANSP code [8]. We are using neutron scattering coefficients from Monte-Carlo neutron transport calculations [18]. The least-squares fit procedure forms the basis for the error analysis, and also allows propagation of errors in fixed model parameters and the study of correlations between errors in free model parameter [26]. The practical implementation of all post-processing and fitting is in the transport analysis package UTC [26] which is otherwise used for impurity transport studies at JET [10].

Tritium can be introduced into the JET tokamak by short, 80msec T_2 gas puffs of up to 6mg using a piezo-crystal valve [14]. The amount that is puffed is measured by the pressure drop in the reservoir of the valve. Globally, the fraction of tritium in the influx is below the spectroscopic detection limit; it would require $\Gamma_T/(\Gamma_D + \Gamma_T)>5\%$ to be measurable. The time evolution of the tritium entering the plasma is instead measured locally with 10msec time resolution from the $T\alpha$ emission using a line-of-sight through the main horizontal port where the valve is installed, see Fig.1. In L-Mode plasmas, or in the presence of small Type III ELMs, the detailed shape of the gas flow can be measured, but in the presence of large Type I ELMs this is not possible. However it turns out that the shape of the puff is invariant in all discharges where it can be measured; specifically it does not depend on the actual amount puffed. Therefore the shape was determined by fitting a curve to the cases where it can be resolved. The only free parameter to fit the $T\alpha$ signal in the presence of Type I ELMs then is the time of the puff, which can be done unambiguously.

The second method to introduce tritium is by a short (typically 200ms) pulse with a T^0 beam (100keV, 1MW) [15]. The neutron emission following the T^0 beam injection is at first dominated by the non-thermal T^+ ions. The deposition profile is peaked on axis, but the time for the thermalised tritium ion density to relax to the final shape is too short for the data from this phase to be useful for the study of transport coefficients, except possibly in the presence of an ITB. The main use of these discharges for transport analysis is the measurement of the rate of decay of the neutron signal after the fast ions have slowed down. This does not in itself provide a measurement of transport coefficients, but serves as a constraint on the analysis of T_2 gas puff shots. Such a constraint is necessary since the rate of decay in T_2 puff discharges, measured after the tritium ion density profile has fully relaxed, is always longer than the rate of decay afterthe T^0 beam injection, see Fig.2. The recycling coefficient,

i.e. the probability for a tritium ion that is lost from the plasma to be reflected from the wall or divertor and return to the plasma, is the same in both discharges. The tail seen on the Tα emission (Fig.1) is too short to account for the longer rate of decay. A different explanation is required.

Following the gas puff, we find about 10% of the tritium that was puffed inside the plasma by the time of peak neutron emission, in contrast to T^0 beam injection which results in near 100% fuelling efficiency. The rest of the tritium after the puff is in or on the vessel wall and divertor tiles. Tritium released from these components acts as a source and is responsible for the delayed decay of tritium from the plasma. If this source was constant in time, the rate of decay would actually be the same as after beam injection, with only a new steady-state value being reached long after the puff. For the analysis of tritium ion transport we do not require a detailed model of neutral tritium pathways and the ionization or transport in the scrape-off layer. We only require a model for the flux in and out of the region observed by the neutron diagnostic. We use a quasi-realistic three-reservoir model (plasma, wall, divertor) with physically plausible free parameters: the fraction of tritium to be deposited on the vessel wall immediately after the T_2 puff, and wall and divertor retention times. The values we need to adopt for these turn out to have physically plausible values; the fraction of tritium to the wall is around 0.6 (from simple arguments like molecular breakup in the scrape-off layer we would expect around 0.5), and typical wall retention times between 0.2 and 0.5 secs are found(which is of the order of the plasma energy confinement time). We know that the divertor retention time is longer than 5 secs because, within the observed time window, the 14MeV yield settles down to a steady level long after the T_2 puff which is larger than the value before the T_2 puff. However these parameters should not be over interpreted. In the end, they are constrained by the need to match the signal recorded in the outermost channels of the neutron profile monitor, and more strongly by the knowledge of the decay time of tritium from the T^0 beam injection partner shot. The latter is imposed during the least-squares fit by only seeking solutions that exhibit the same decay rate.

2. DETAILED OBSERVATIONS BASED ON 14 MEV NEUTRON EMISSION

Shortly after the T^2 puff (≈150msec), the tritium ion density is hollow and the 14MeV neutron emission is due to interaction with fast deuterium ions deposited in the outer plasma region by deuterium neutral beam injection. Due to the geometry of the JET beams, ions are injected into trapped orbits for r/a>0.3, and since the 14MeV neutron emission is dominated by fast ions at the upper end of the energy distribution the 14MeV emissivity contours have a crescent shape, as illustrated in Fig.3. Also passing ions (borninboard on the second pass of the beam through the plasma, or those scattered into initially marginally passing orbits) have a poloidally asymmetric distribution. Once the tritium density profile has relaxed, the 14 MeV emissivity contours are peaked on axis, where thermal-thermal reactions become important and most fast ions are passing. The 2.5MeV emissivity contours are always peaked. (Note that tomographic inversion of the is only possible after integration of the signal in time, and by restricting the class of functions for the tomography algorithm. Thus these images are useful as illustrations, but cannot be used for transport analysis. Instead, we reconstruct the original line integrals from a transport model as described in Section 2).

Sawtooth collapses result in tritium density profile changes [25]. The dominant contribution to the observed changes of the neutron line integrals is the redistribution of fast deuterium ions. At the time when they disappear from the central channels (evident from a dip in the central line integrals), a burst of 14MeV neutrons is seen in channels with an impact parameter as far as r/a ≈ 0.5. It is interesting to note that sawtooth collapses that occur during inward propagation of tritium, i.e. shortly after the puff, do not exhibit this feature: the ejection of deuterium ions from the core is compensated by the tritium ions being swept into the core, keeping the line integrals almost constant. The magnitude of the effects from sawteeth are most pronounced at low density, because the fast deuterium ion density is more peaked. As the electron density increases, the beam deposition profile becomes wider and the difference between the deposition profile and the flattened profile following the sawtooth collapse is reduced.

The effect of Neo-classical Tearing Modes (NTM) has been studied in pairs of discharges with near identical plasma conditions, one with and one without a 3/2 NTM [11]. Changes to 14MeV line integrals are observed for lines-of-sight with an impact parameter inside the region of q<3/2. The discharge with NTMs has slightly reduced temperature and density, and at least some part of the difference can be explained by these. The remainder requires a change in the tritium transport, localized at, or within, the q=3/2 surface. Both changes in D_T and v_T are consistent with the observations, but the effect of the NTM on the fast ions (which are mainly responsible for the neutron emission in this region) requires further modeling before a firm conclusion is possible.

ELMs that occur during the time of the puff result in a small increase of 14 MeV line integrals with an impact parameter as far into the plasma as r/a≈0.5msec within 10msec. We do not have a quantitative understanding of this effect, but it can be shown that changes in ELM frequency should result in changes to the fuelling efficiency of tritium on the assumption that D_T during an ELM rises significantly above the level of D_T between ELMs [1]. The transient effects could be the result of deeper fuelling due to charge-exchange which would be a result of the increase of the deuterium neutral flux after the ELM (at the same time losses due to charge-exchange also increase; this means that it is either less important than the deeper fuelling or deeper fuelling due to charge-exchange is not the correct observation). Furthermore it is possible that there is an increase of tritium neutral influx as a result of energy or particles released from the plasma during the ELM dislodging tritium from the wall or divertor. A combination of all three effects (transient changes in transport coefficients near the edge, and the presence of more tritium ions combined with more efficient deeper fuelling) may be the answer, but this will require fitting of transport simulations with changes in transport coefficient, sources and sinks on a 1-10μsec time scale to the data to be confirmed.

3. TRITIUM TRANSPORT NEAR NEO-CLASSICAL LEVELS AND SCALING OF TRITIUM TRANSPORT

Tritium transport remains well above neo-classical levels in most cases we studied. We have seen tritium transport approach neo-classical levels under two circumstances: at high density in high current, low q_{95} discharges [1] (Fig.4) and in the transport barrier region of ITB discharges [19] (Fig.5).

In high density discharges, the measured diffusion coefficient D_T remains above neo-classical for r/a>0.5, and we find $D_T/\chi_{eff}\approx 3$ in this region which is the lowest ratio found in any of the discharges we studied. Tritium transport agrees with neo-classical predictions performed with the NCLASS code [12] for r/a<0.5. Also shown in Fig. 4 is the neo-classical prediction for D_D which demonstrates that neo-classical effects are qualitatively and quantitatively different for minority and majority fuel ion species, specifically the difference between D_T and D_D well exceeds the difference due to the mass ratio. The reason for this is that a deuterium and tritium ion can exchange place after a Coulomb collision, which is important for the minority species but makes only a small contribution for the majority species. This transport can take the form of diffusive and convective transport, noting that v_T and v_D are both very small and the only important difference in the neo-classical predictions is the difference between D_T and D_D.

In ITB discharges, we observe three features: a reduction of D_T to neo-classical values in the transport barrier, an increase of D_T in the region enclosed by the barrier to large values, and a reduction of v_T in the barrier but not quite to neo-classical values, see Fig.5. Without the reduction of D_T in the barrier more tritium would reach the core than observed, while the increased D_T in the region enclosed by the barrier speeds up the rate of rise to peak emission and the rate of decay after the peak emission for the inner-most channels in agreement with the measured line integrals. Establishing the correct value for v_T in the barrier is more subtle: assuming the convection is neo-classical, the correct rate of rise can be obtained, but the rate of decay would be too fast. Thus the correct rate of transport into as well as out of the region enclosed by the barrier requires a combination of neo-classical D_T and reduced but still above neo-classical v_T.

For the scaling of transport, we will mainly focus on the edge of the region observed by the neutron cameras, i.e. r/a = [0.65,0.80]. In the central region, differences between ELMy H-Mode discharges (q_0<1 exhibiting sawtooth behaviour), hybrid scenarios ($q_0 \approx 1$)and weak as well as strong ITB discharges (q_0>2 or even q_0>3) can be expected. As a working hypothesis, tritium transport well outside the central region should be comparable between all scenarios.

As is shown in Fig.6, there is a strong correlation for all three scenarios of D_T with q_{95} for r/a=[0.65,0.80]. The variation of q_{95} in the data has been obtained by varying current as well as field, which is shown in the inset figure. At the same time energy transport, characterized by ceff, is not strongly affected and thus the ratio D_T/χ_{eff} varies between 0.3 and 2.0 from high density, low q_{95} to low density, high q_{95} (most of the discharges in this database do not allow an accurate separation into ci and ce). There is however considerably more variation in the scaling of D_T/χ_{eff} with q_{95} than in the scaling of D_T with q_{95} alone; specifically plasmas with Ion Cyclotron Resonance Heating (ICRH) have a larger ratio of D_T/χ_{eff}. Since we have only analysed three discharges with ICRH heating at high density and low q_{95} so far we cannot be sure if this observation holds at all densities and values of q_{95} or indeed for all high density, low q_{95} discharges.

The correlation of D_T is better with the local value of q, calculated by EFIT [16] which suggests that the orbit width of trapped particles is an important parameter determining the scaling. Therefore we show in Fig.7 the relationship of the normalized diffusion coefficient $D_T/B\phi$ [4] with the normalized

poloidal Larmor radius $\rho^*_{pol} = q \times \rho^*$. This results in a very strong correlation for the ELMy H-Mode discharges alone, which is better described by gyro-Bohm scaling (ρ^{*3}_{pol}) rather than Bohm scaling (ρ^{*2}_{pol}). However with ρ^*_{pol} as ordering parameter a difference appears for hybrid scenario discharges and for discharges with significant ICRH heating, whereas the two ITB discharges agree with the trend within errors. Also shown in the inset of Fig.7 is an equally strong correlation of $v_T/B\phi$ with local ρ^*_{pol}. In this figure, the hybrid scenario discharges follow the trend of the ELMy H-Mode discharges, whereas the ITB discharges stand out. The ratio of v_T/D_T, which determines the profile shape, varies from $-2\ m^{-1}$ for high q, low density to $\pm 0.1 m^{-1}$ for low q, high density.

The dedicated scans of ν^* and β at fixed $q_{95} = 3$ result in the data points in Fig.7 that deviate from the trend line for ELMy H-Modes at low ρ^*_{pol}, while the hybrid scenario discharges are characterised by larger β. Regression analysis shows that collisionality, ν^*, is not important, but there is an inverse dependence on β which is in contrast to energy transport for which a weak dependence on ν^* and no dependence on β is found [21, 2]. We note that an inverse dependence on β has been found on DIII-D for helium particle transport [22].

SUMMARY AND CONCLUSIONS

Tritium transport experiments have been performed in identical pairs of discharges with on axis T^0 beam injection and T_2 gas puffs at the edge. The rate of decay of the thermalised tritium following the T^0 beam injection is used as a constraint on the analysis of the T_2 gas puff discharges, i.e. only solutions are sought in the least-squares fit that exhibit the same decay rate. This allows the time dependence of the tritium influx from vessel wall and divertor after the T_2 gas puff to be inferred at the same time as the radial profiles of the transport parameters D_T and v_T for r/a<0.85 are determined. The leading edge and thus the exact time of the influx is measured from local observation of $T\alpha$ emission using a line-of-sight through the main horizontal port where the valve is installed.

The initially hollow 14MeV emissivity contours after T_2 gas puffs are explained by the poloidal distribution of fast deuterium ion orbits from neutral beam injection. Sawtooth events redistribute these fast ions radially and, when the thermal tritium ion density is peaked at the time of the collapse, result in dips of neutron emission for central chords at the same time as chords at $r/a \approx 0.5$sec see n increase. During inward propagation of tritium, the two redistribution events can cancel each other out such that only small changes are seen on 14 MeV line integrals. NTMs have been seen to cause changes to tritium transport at, or within, the q=3/2 surface where the mode is located, however the effect of the mode on fast deuterium beam ions remains to be clarified. ELMs cause a small increase in neutron line integrals within 10 msec at r/a≈ when they occur during the T_2 gas puff, a quantitative understanding of this observation remains to be established.

Tritium diffusion can approach neo-classical levels in two cases: in the core of high density ELMy H-Mode discharges at low q_{95} and in the transport barrier region of ITB discharges. In the first case, the measured tritium convection is consistent with neo-classical predictions, however for ITBs it is not. Under all other conditions studied, the transport is well above neo-classical. The measured D_T and v_T for the edge of the plasma region observed by the JET neutron profile monitor,

r/a=[0.65,0.80], show a strong correlation with q_{95} which is consistently seen for ELMy H-Mode, hybrid scenario and ITB discharges. This correlation is also reflected in the ratio of DT/ceff which varies between 0.3 and 2.0 from high density, low q_{95} to low density, high q_{95}. An analysis of the dependence of DT on the normalised poloidal Larmor radius ρ^*_{pol} supports a gyro-Bohm scaling, but there is a need for at least one other local plasma quantity to establish a consistent scaling. We find that ν^* does not play a role, but there is an inverse b dependence, which is in constrast to energy transport where negligible b dependences have been observed in dedicated scans.

ACKNOWLEDGEMENTS

This work was performed under the European Fusion Development Agreement, and partly funded by the UK Engineering and Physical Sciences Research Council and by EURATOM.

REFERENCES

[1]. Belo P. et al. "Role of impurity and deuterium fuelling in evolution of trace tritium in JET ELMy H-mode: transport analysis and predictive modelling", Proc. 31st EPS Conference on Plasma Physics, London 2004, P1-169

[2]. Cordey J.G. et al, "The Scaling of the Energy Confinement and Transport in JET ELMy H-Modes with the Dimensionless Physics Parameters", Proc. 31st EPS Conference on Plasma Physics, London 2004, O1-05

[3]. Connor J.W. et al., Nucl. Fusion **44** (2004) R1

[4]. Connor J.W. and Taylor J B, Nucl. Fusion **17** (1977) 1047

[5]. Efthimion P. et al. Phys. Rev. Letters **55** (1995) 85

[6]. Efthimion P. et al. Nuclear Fusion **39** (1999)

[7]. Greenwald M. et al. Nuc1ear Fusion **28** (1988) 2199

[8]. Goldston R. et al. J. Comput. Phys. **43** (1994) 93

[9]. JET Team, presented by K-D Zastrow, Nuclear Fusion **39** (1999) 1891

[10]. Giroud C. et al. "Z-dependence of impurity transport in steady-state ITB and Hybrid scenario at JET". Proc. 31st EPS Conference on Plasma Physics, London 2004, P1-144

[11]. Hender T.C. et al. "Trace-Tritium Measurement of Magnetic Island Effect on Particle Confinement", Proc. 31st EPS Conference on Plasma Physics, London 2004, P1-163

[12]. Houlberg W. et al. Nucl. Fusion **34** (1994) 93

[13]. Joffrin E et al. Plasma Phys. Contr. Fusion **44** (2002) 1203

[14]. Jones T.T.C. et al. "Technical and scientific aspects of the JET Trace-Tritium experimental campaign", 7th Tritium Science and Technology, 12/9/-17/9/04, Baden-Baden, Germany

[15]. Surrrey E. et al., "Neutral Beam Injection in the JET Trace Tritium Experiment", 7th Tritium Science and Technology, 12/9/-17/9/04, Baden-Baden, Germany

[16]. Lao L.L., et al., Nucl. Fusion **30** (1990) 1035

[17]. Lauro-Taroni L. et al. Proc. 21st EPS Conference on Contr. Fusion and Plasma Physics, Montpellier, Vol I, p. 102

[18]. Loughlin M. et al. Rev. Sci. Instrum. **70** (1999) 1123
[19]. Mailloux J. et al. "Tritium Fuelling of JET plasmas with Internal Transport Barriers", Proc. 31st EPS Conference on Plasma Physics, London 2004, P1-148
[20]. Matthews G.F. et al. J. Nucl. Mater. **266-269** (1999) 153
[21]. McDonald D.C. et al, Plasma Phys. Contr. Fusion 46 (2004) A215
[22]. Petty C.C. et al. Phys. Plasmas **11** (2004) 2514
[23]. Popovichev S. et al. "Performance of Neutron Measurements during Trace Tritium Experiments on JET", Proc. 31st EPS Conference on Plasma Physics, London 2004, P5-173
[24]. Rebut P.H., Nucl. Fusion **32** (1992) 187
[25]. Voitsekhovitch I. et al. "Transport analysis of trace Tritium experiments on JET and comparison with theory-based transport models", Proc. 31st EPS Conference on Plasma Physics, London 2004, P1-158
[26]. Whiteford A.D. et al. "Quantitative forward modelling of neutron emission to derive transport coefficients of tritium in JET, including error propagation through to transport parameters", Proc. 31st EPS Conference on Plasma Physics, London 2004, P1-159
[27]. Wolf R.C., Plasma Phys. Contr. Fusion **45** (2003) R1

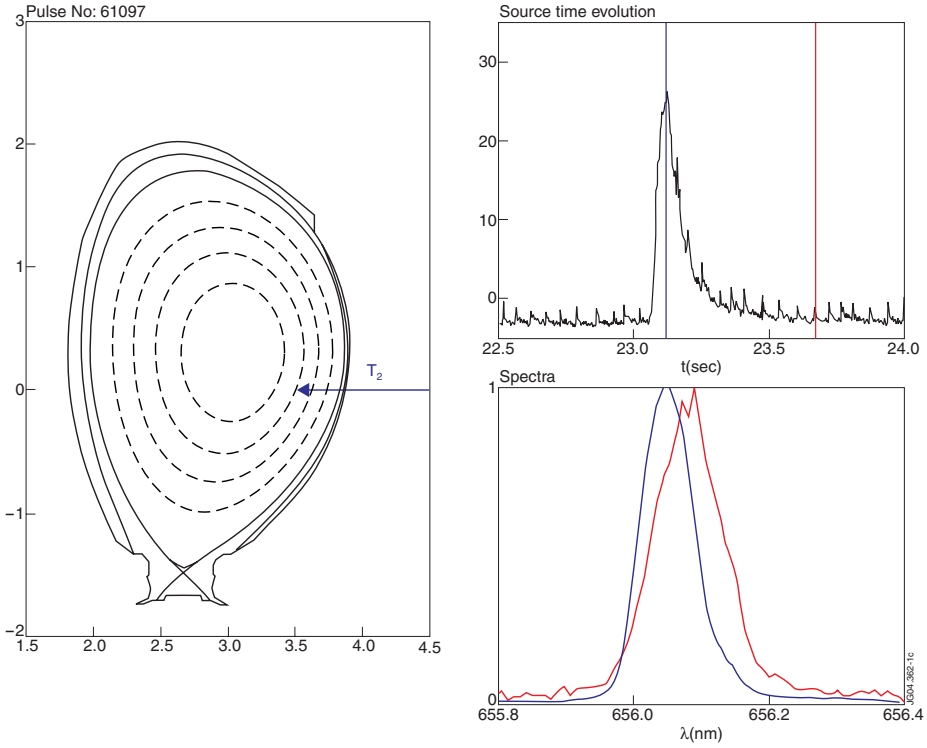

Figure 1: Tritium is puffed from a main horizontal port in the midplane. The time of the puff is measured by analyzing the local increase in Tα emission at 656.04nm (top right), which is detected along a line-of-sight through the same port as indicated in the figure on the left. Before the puff, the spectrum of the D_α emission at 656.10nm from inboard and outboard is seen simultaneously, and thus shows the Zeeman splitting at two different magnetic fields (bottom right). The width of the Tα emission is only affected by the outboard magnetic field and therefore the spectral line is narrower.

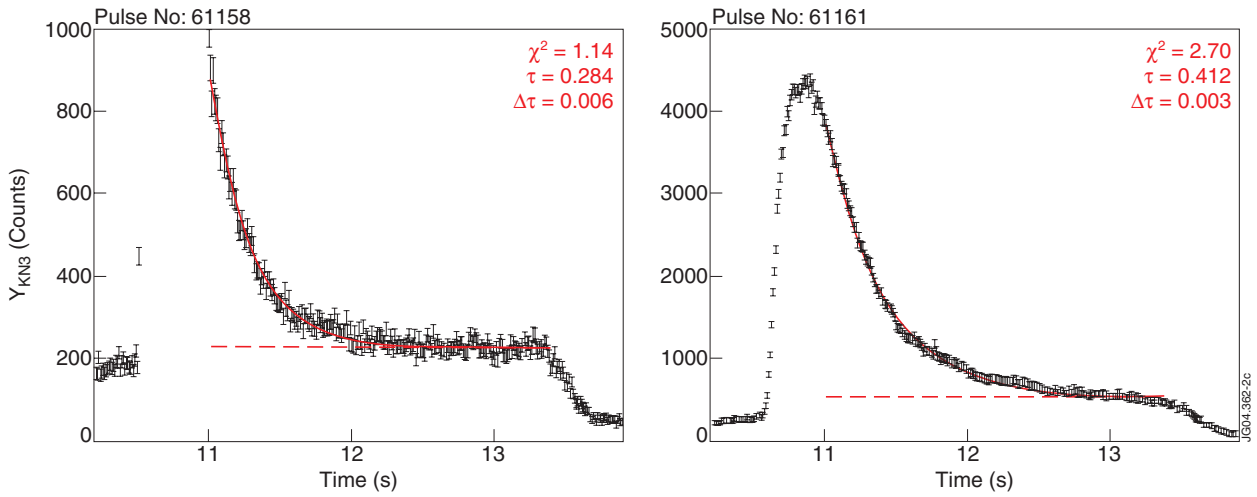

Figure 2. Decay of the 14MeV neutron signal following T^0 beam injection (left) and a T_2 gas puff (right) in two identical discharges. The emission due to fast T ions is much stronger, and the data from this phase are not shown in the figure on the left. After the T ions have thermalised we measure the decay time constant, for this particular hybrid scenario discharge we obtain 0.284±0.006 sec. The decay time constant following the T_2 gas puff is longer, 0.412±0.003 sec in this case, because the source continues to evolve.

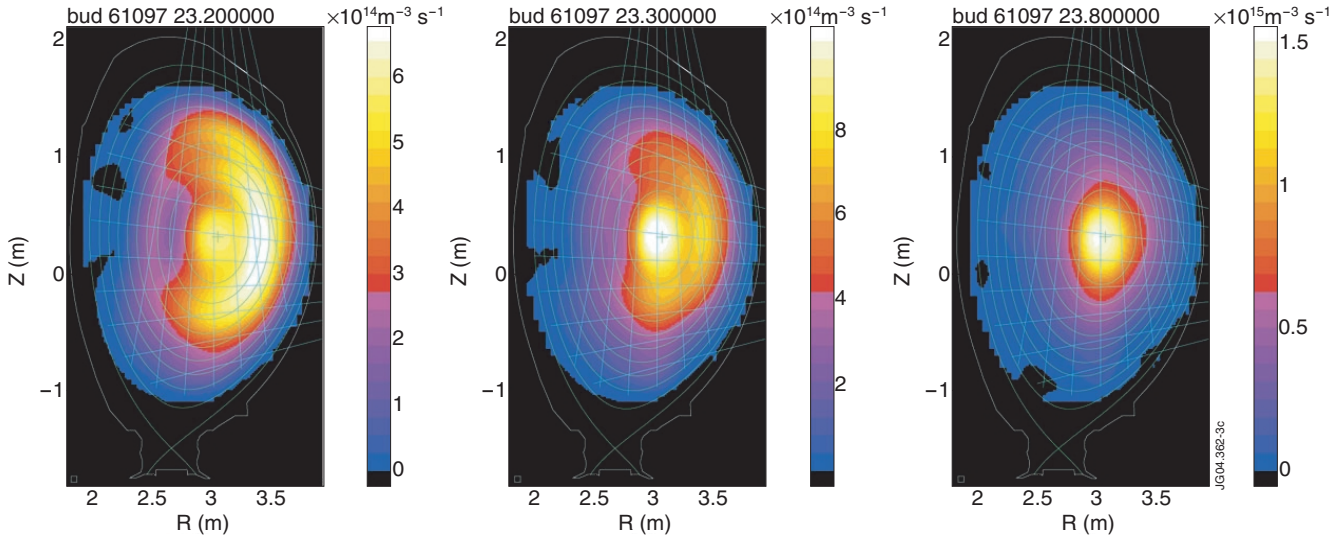

Figure 3: Comparison of 14MeV emissivity contours 150msec after the puff, when the tritium density is hollow (left), with the contours after 250msec (middle) and the peaked shape after 75msec (right) once the tritium density profile has fully relaxed. The initial crescent shape is due to the poloidal distribution of fast deuterium ions from beam injection. Note that these reconstructions are for illustrative purposes only and are not used in the tritium transport analysis.

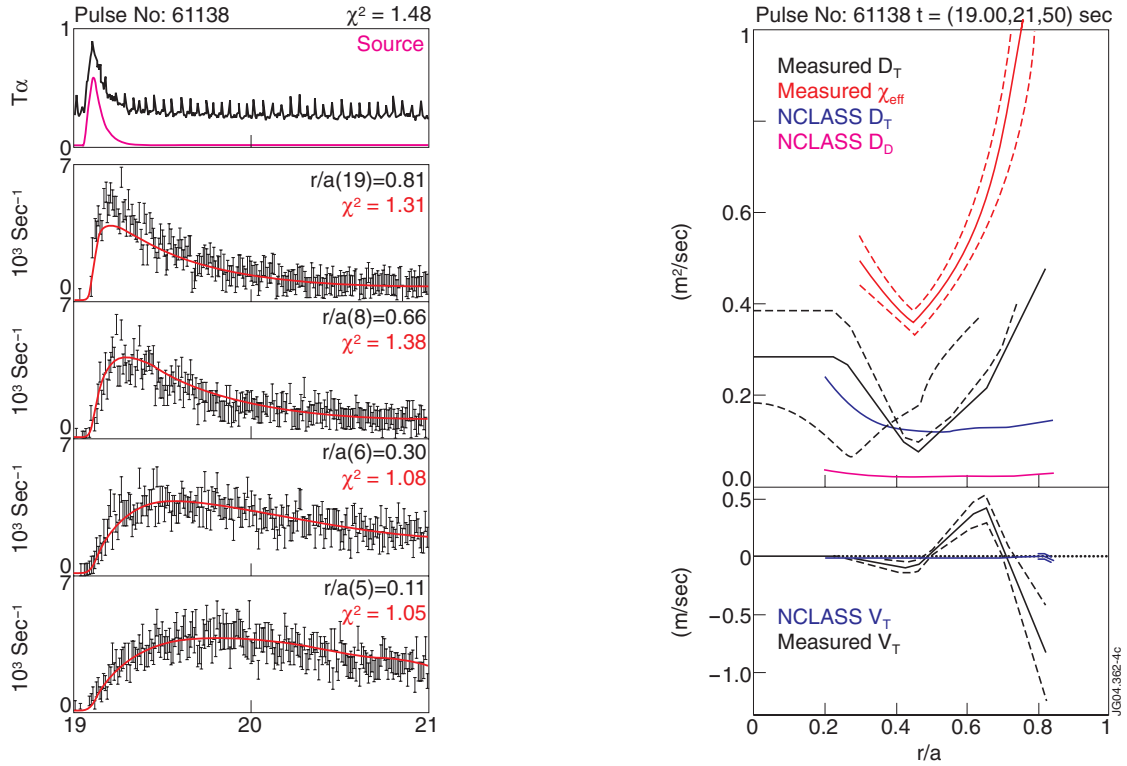

Figure 4: Example of tritium transport analysis at high density and low q_{95}. The time evolution along four individual chords of the neutron profile monitor is shown covering the range from the edge of the observed region to the core (the fit is performed to all nineteen channels). The top frame on the left shows the D_α and T_α emission (Fig.1) and the influx derived from it. For this example, the tritium diffusion and convection coefficients approach the neo-classical values for r/a<0.5. For r/a>0.5 diffusion and convection are above neo-classical. We find $D_T/\chi_{eff}\approx 3$ in this region, which is the lowest ratio found in any of the discharges we studied.

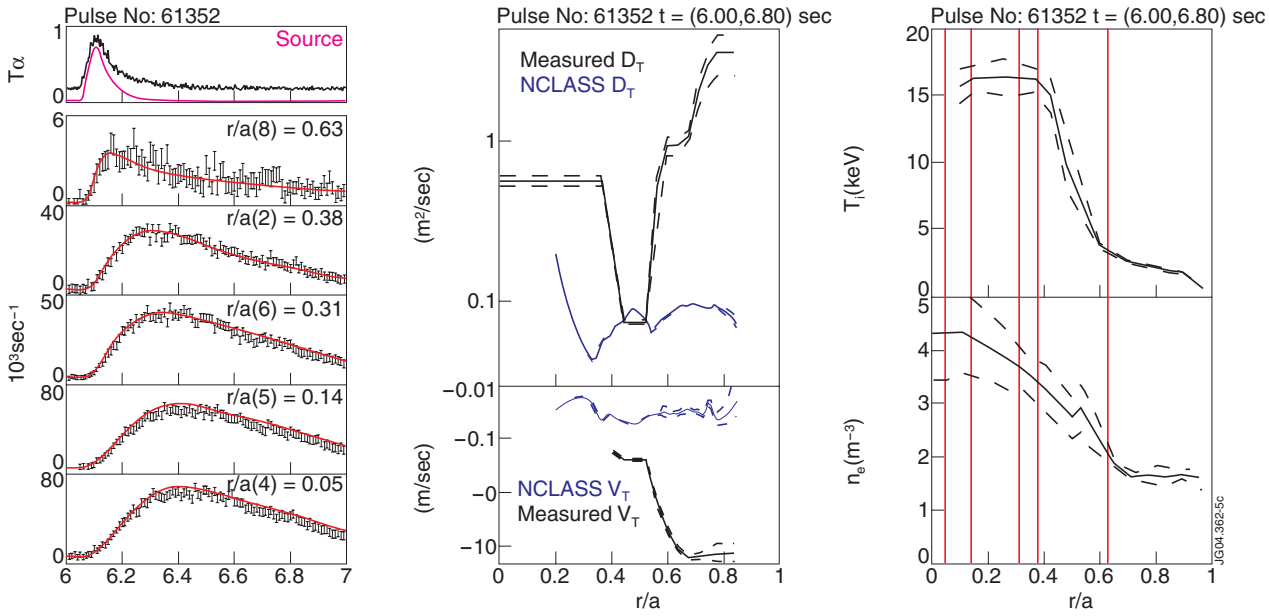

Figure 5: In discharges with a strong ITB, the diffusion coefficient in the barrier drops to neo-classical values, while the inward convection is reduced but not quite to neo-classical, as illustrated in the figure in the middle. In the region enclosed by the barrier, the diffusion coefficient is increased. The figure on the left shows the best fit solution (for a chord with an impact parameter just outside the barrier, two just inside, and two near the plasma axis). The figure on the right shows the relationship of these chords with the average ion temperature and electron density during the analysed time interval.

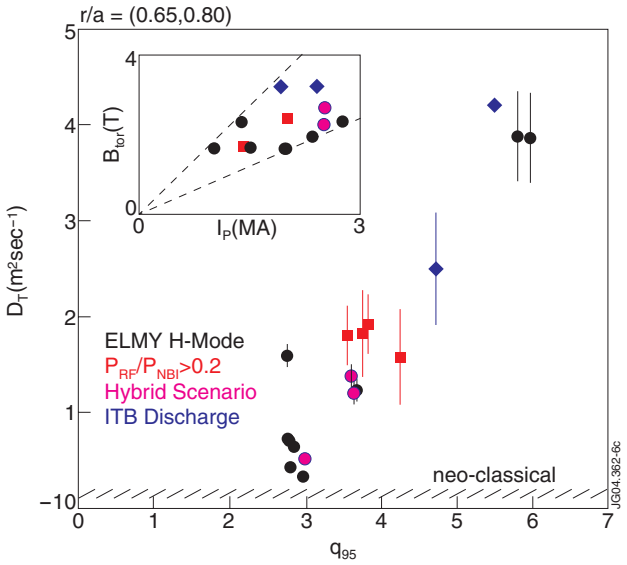

Figure 6: A strong trend for increased D_T for r/a=[0.65,0.80] with q_{95} is observed for all three operational scenarios. The shaded region indicates the typical range of diffusion coefficients from neo-classical calculations. The variation in q_{95} has been obtained by variation of toroidal field as well as plasma current, as is shown in the inset figure.

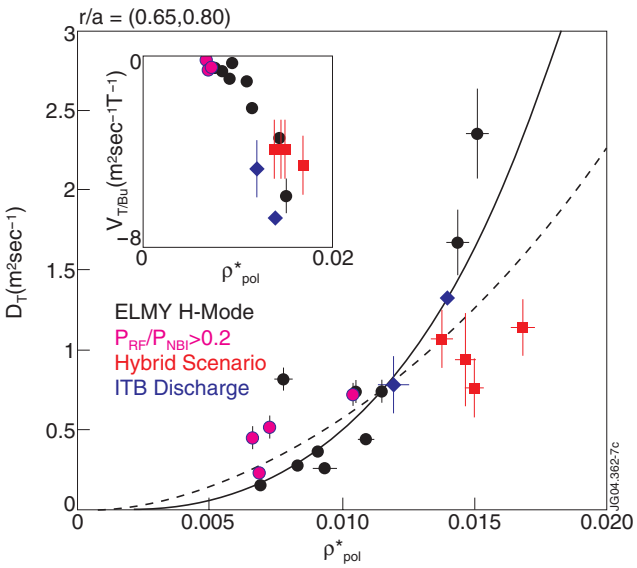

Figure 7: Plot of the normalised D_T/B_ϕ and v_T/B_ϕ against local poloidal Larmor radius, ρ^*_{pol}. The solid line corresponds to gyro-Bohm scaling ($\rho^*_{pol}{}^3$), the dashed line to Bohm scaling ($\rho^*_{pol}{}^2$). In contrast to Fig.6, differences between hybrid scenario discharges and ELMy H-Mode and ITB discharges appear in DT/B f, and differences between ITB discharges and the other two operational regimes appear in v_T/B_ϕ. While there is a strong correlation with ρ^*_{pol}, additional local plasma parameters are required to explain the observed trend as well as the deviations from it (see text for details).